

Estimating the Treatment Effects of Multiple Drug Combinations on Multiple Outcomes in Hypertension

Ruoqi Liu¹, Lang Li², and Ping Zhang^{1,2,3,*}

¹Department of Computer Science and Engineering. The Ohio State University, 2015 Neil Ave, Columbus OH 43210, USA.

²Department of Biomedical Informatics. The Ohio State University, 1800 Cannon Drive, Columbus OH 43210, USA.

³Translational Data Analytics institute. The Ohio State University, 1760 Neil Ave, Columbus OH 43210, USA.

*Corresponding Author & Lead Contact: zhang.10631@osu.edu

Summary

Hypertension poses a significant global health challenge, and its management is often complicated by the complexity of treatment strategies involving multiple drug combinations and the need to consider multiple outcomes. Traditional treatment effect estimation (TEE) methods struggle to address this complexity, as they typically focus on binary treatments and binary outcomes. To overcome these limitations, we introduce **METO**, a novel framework designed for TEE in the context of multiple drug combinations and multiple outcomes. **METO** employs a multi-treatment encoding mechanism to handle multiple drug combinations and their sequences effectively, and differentiates between effectiveness and safety outcomes by explicitly learning the outcome type when predicting the treatment outcomes. Furthermore, to address confounding bias in outcome prediction, we employ an inverse probability weighting method tailored for multiple treatments, assigning each patient a balance weight derived from their propensity score against different drug combinations. Our comprehensive evaluation using a real-world patient dataset demonstrates that **METO** outperforms existing TEE methods, with an average improvement of 5.0% in area under the precision-recall curve and 6.4% in influence function-based precision of estimating heterogeneous effects. A case study demonstrates that our method successfully identifies personalized optimal antihypertensive dual regimens, achieving maximal efficacy and minimal drug-related safety risks. This showcases its potential for improving treatment strategies and outcomes in hypertension management.

Keywords

Treatment effect estimation, deep learning, real-world data, hypertension, multiple drug combinations, precision medicine

Introduction

Hypertension is a major global health issue, responsible for around 7 million deaths and 57 million disabilities annually^[1]. However, optimal blood pressure control remains elusive for roughly 70% of patients, primarily due to inadequate implementation of combination therapies^[2]. The challenge lies in selecting effective antihypertensive treatment strategies^[3], including the choice between starting with monotherapy and gradually adding another drug (stepped-care) or beginning with a drug combination^[4,5].

This introduces a pivotal medical question: “How can we determine the most effective antihypertensive drug combinations (treatments) to improve hypertension-related conditions (outcomes)?” Tackling this question requires an exploration into the complex landscape of treatment options, encompassing a variety of drug combinations and sequences. Moreover, the imperative for a thorough evaluation of treatments underscores the inherent tension between effectiveness and safety outcomes in hypertension^[6], illuminating the dual, often opposing, dimensions of outcome assessment^[7].

43 Treatment effect estimation (TEE), which identifies the causal effects of *treatments* on the patient
44 *outcomes*, can be leveraged to address the above complex question of optimizing antihypertensive drug
45 combinations. However, existing TEE approaches, designed predominantly for binary treatments and
46 binary outcomes⁸⁻¹⁰, struggle with multiple treatments and multiple outcomes. Some approaches¹¹⁻¹⁴
47 extend existing models for multiple treatments by directly increasing treatment arms, thus facing efficiency
48 and generalizability challenges¹⁵. Others improve adaptability using unified treatment embeddings for
49 multiple treatments^{15,16}. Nevertheless, significant challenges remain in applying these methods to TEE
50 with multiple treatments and multiple outcomes, particularly for antihypertensive drug combinations.

51 First, existing methods^{13,16} typically treat all treatments uniformly, without utilizing the nuanced details
52 of each. This lack of granular differentiation limits their practicality, especially in the studied scenarios
53 where the combination and sequential administration of drugs are crucial. Second, while some stud-
54 ies¹⁷⁻¹⁹ have explored TEE in the context of multiple outcomes, they are mainly designed for randomized
55 controlled trials without adjustment for confounding bias, and more importantly, fail to differentiate between
56 outcome types (i.e., therapeutic effectiveness versus adverse effects). In addition, different outcomes can
57 have different relationships with the covariates and treatments. Failing to consider such various rela-
58 tionships may lead to confounding bias and inaccurate treatment effects estimation. Finally, there is a
59 noticeable gap in the literature regarding the comprehensive treatment effect assessment tool that facili-
60 tates clinical decision-making.

61 To address these challenges, we propose a novel framework, called **METO**, to estimate the treatment
62 effects of **M**ultiple drug combinations on **m**ulTiple **O**utcomes for identifying optimal antihypertensive drug
63 combinations (see Fig. 1). First, we address the complexities of multiple drug combinations through the
64 proposed multi-treatment modeling. This mechanism processes the detailed information of drug com-
65 binations and administration sequences independently, before synthesizing these elements via a deep
66 fusion layer. Second, we leverage the specific outcome type information as additional guidance to differ-
67 entiate between effectiveness and safety outcomes, enhancing the accuracy of outcome prediction. In
68 addition, to address confounding bias in outcome prediction, we employ an inverse probability weight-
69 ing method tailored for multiple treatments, assigning each patient a balance weight derived from their
70 propensity score against different drug combinations. Our comprehensive evaluation shows that METO
71 outperforms existing treatment effect estimation methods and successfully identifies personalized optimal
72 drug combinations with beneficial effects and reduced safety risks.

73 Our contributions are summarized as follows:

- 74 • **Problem.** We address the challenge of TEE in hypertension management, focusing on multiple drug
75 combinations and their impact on both effectiveness and safety outcomes.
- 76 • **Method.** We propose **METO**, a novel method that incorporates multi-treatment encoding and explicit
77 outcome-type learning to handle complex drug combinations and differentiate between effectiveness
78 and safety outcomes.
- 79 • **Experiments.** We validate **METO**'s superior performance against existing TEE methods using a large-
80 scale real-world dataset and demonstrate its practical efficacy through a case study on personalized
81 drug combination recommendation.

82 Results

83 Overall Framework

84 We develop an end-to-end treatment effect estimation framework that can be utilized for recommend-
85 ing optimal drug combinations for patients with hypertension. As shown in Fig. 1, the patient medical
86 records are extracted from an observational database and then processed into drug combination cohorts
87 for comparing treatment effectiveness. The treatment effects are estimated with the proposed **METO**,
88 which is designed specifically for the scenario of multiple treatments and multiple outcomes. Finally, op-
89 timal drug combinations are suggested by assessing the treatment effects across both effectiveness and
90 safety outcomes.

91 Dataset

92 We collect data on approximately 130 million patients from the MarketScan Commercial Claims and En-
93 counters (CCAЕ)¹ database, covering the period from 2012 to 2021. This dataset contains individual-level,
94 de-identified healthcare claims information from employers, health plans, and hospitals. We extract more
95 than 19 million patients who are diagnosed with hypertension (Appendix Table A1). Within this patient
96 cohort, we identify more than 11 million patients who have at least one risk factor (i.e., subclinical organ
97 damage, diabetes, renal, or associated cardiovascular disease)²⁰ and initiated first-line antihypertensive
98 drugs. Each patient record consists of demographics (e.g., age and sex), co-morbidities (via ICD-9/10
99 diagnosis codes) as well as co-prescribed medications (using national drug codes [NDC]). For uniformity,
100 ICD-9/10 codes were consolidated into a standardized coding schema using the clinical classifications
101 software (CCS)². Figure 2 displays the dataset’s statistics including the distribution of overall population,
102 age, gender, and outcome across different drug combinations, respectively. Figure 3 illustrates the de-
103 tailed study design for each treatment cohort, including treatment definitions, computation of confounding
104 variables, and outcomes. The flowchart of the user cohort selection is provided in Appendix Fig. A1.

105 **Treatments.** Following hypertension management guidelines³, we categorized first-line antihypertensive
106 agents into thiazide diuretics (TZDs), ACE inhibitors (ACEIs), angiotensin receptor blockers (ARBs), and
107 calcium channel blockers (CCBs). We identified five distinct first-line drug combination regimens, each
108 comprising two different classes: (1) TZDs and ACEIs; (2) TZDs and ARBs; (3) TZDs and CCBs; (4)
109 ACEIs and CCBs; (5) ARBs and CCBs. We note that ACEIs and ARBs are not combined in clinical
110 practice. These combinations also varied by assignment order: initial combination (less than 30 days
111 between first and second drug initiations) and stepped-care (between 30 and 180 days). We identified
112 a total of 15 unique drug combinations, considering both the specific combinations and their order of
113 assignment. Detailed definitions of these drugs are provided in Appendix Table A2.

114 **Outcomes.** Six important outcomes are computed during the follow-up period after the treatment initial-
115 ization, including three primary effectiveness outcomes (stroke, acute myocardial infarction [MI], heart fail-
116 ure [HF]) and three safety outcomes (acute kidney failure [AKF], gout, venous thromboembolism [VTE]).
117 These outcomes are chosen based on their significance in hypertension management guidelines³ and
118 insights from recent large-scale studies in hypertension⁶. Outcome occurrences are identified using di-
119 agnosis codes, with detailed definitions available in Appendix Table A3.

120 **Confounders.** A comprehensive list of potential confounders is compiled, including demographics (age
121 and gender), 282 unique co-morbidities (based on diagnosis codes), and 1,378 unique co-prescribed
122 medications. These confounders, relevant to both treatment assignment and outcomes, are assessed
123 during the baseline period before treatment initiation.

124 Baselines and Setup

125 In the experiments, we compare our method with state-of-the-art baselines, which can be classified into
126 three main categories:

- 127 • *Basic meta-learners:* (1) **S-learner** is a meta-learner²¹ that builds a binary outcome prediction model
128 for all treatment groups; (2) **T-learner** is also a meta-learner²¹ that builds multiple outcome prediction
129 models for each treatment group separately.
- 130 • *TEE methods for binary treatments and binary outcomes:* (1) **TARNet**⁸ predicts the potential outcomes
131 based on balanced representations between treated and controlled groups; (2) **DragonNet**⁹ jointly
132 predicts treatment and outcomes based on the shared representations via a three-head neural network.
- 133 • *TEE methods for multiple treatments and binary (multiple) outcomes:* (1) **PerfectMatch**¹¹ augments
134 samples within a batch with their propensity-matched nearest neighbors. The framework can be natu-
135 rally extended to multiple treatments by matching with the nearest neighbors from each treatment group;
136 (2) **TECE-VAE**¹⁶ incorporates latent variables and causal structure through a variational autoencoder,

¹<https://www.merative.com/real-world-evidence>

²<https://hcup-us.ahrq.gov/toolssoftware/ccs/ccs.jsp>

137 and models multiple treatments with a task embedding; (3) **MEMENTO**^[13] is a direct extension of TAR-
138 Net^[8] to multiple treatments by increasing the number of model branches to the number of treatments;
139 (4) **LR-learner**^[22] adopts a neural network to learn embeddings for individuals and treatments, which
140 are then transformed by a linear operator to predict outcomes based on the dot product of these em-
141 beddings; (5) **TransTEE**^[15] embeds multiple treatments and covariates into a shared hidden space via a
142 Transformer to improve the model’s flexibility and robustness; (6) **NCoRE**^[12] models the cross-treatment
143 interactions by encoding each treatment arm separately and then applying a merge layer to connect all
144 the treatment arms.

145 Note that we implement the S-learner and T-learner with a logistic regression (LR)-based estimator. TAR-
146 Net^[8] and DragonNet^[9] are representative works in TEE but initially designed for binary treatment scenar-
147 ios. We extend these two methods to multiple treatment scenarios as done in^[11]. For baselines originally
148 developed for binary outcomes, we have facilitated their application to multiple outcome contexts by tran-
149 sitioning from a binary classification head to one capable of multi-label classification.

150 **Evaluation Metrics** We evaluate the performance of factual outcome prediction by measuring the area
151 under the Precision-Recall curve (AUPR), focusing on the precision-recall trade-off due to the potential
152 imbalance between positive and negative outcome labels. As the ground truth treatment effects are not
153 observed (i.e., any patient is ever only assigned to one of the treatments in practice), we can not di-
154 rectly compute the traditional metric precision in estimating heterogeneous effects (PEHE)^[23]. Instead, we
155 adopt a recent proxy metric for counterfactual evaluation, called influence function-based precision of esti-
156 mating heterogeneous effects (IF-PEHE)^[24], which measures the mean squared error between estimated
157 treatment effects and approximated true treatment effects (see detailed computation of IF-PEHE [IP] in
158 Appendix C.2). The original metric is designed for binary treatments and binary outcomes, we extend it
159 to multiple treatments and multiple outcomes (MM-IP) as below:

$$\frac{1}{U} \sum_u \left[\frac{1}{|\mathcal{A}| \times |\mathcal{O}|} \sum_{\substack{i,j,q,r \in \mathcal{A} \\ o,s \in \mathcal{O}}} \text{IP}[\hat{\tau}_k^u(\mathbf{a}_{i,j}^o, \mathbf{a}_{q,r}^s), \tau_k^u(\mathbf{a}_{i,j}^o, \mathbf{a}_{q,r}^s)] \right] \quad (1)$$

160 where U is the total number of patients, τ_k^u denotes the treatment effect for patient u on outcome k .

161 **Implementation Details** The dataset is randomly split into training, validation, and test sets with percent-
162 ages of 80%, 10%, and 10% respectively. The number of training epochs is 10 and the learning rate
163 is $5e-5$. The backbone model architecture is a 12-layer Transformer, with 768 hidden units, 12 attention
164 heads, and 3072 for the intermediate size. The parameter β in multi-treatment modeling is set to 0.6. The
165 parameter η in outcome type-informed prediction is set to 1 for the training and 0 for the inference. The
166 parameter λ , which adjusts the influence of treatment prediction, is set to 1. All results are reported on the
167 test sets over 20 initializations of the model. More implementation details including the parameter tuning,
168 training setup, and additional configurations are mentioned in Appendix C.3.

169 Overall Performance Comparison

170 Results in Table 1 present a comparative evaluation of our proposed **METO**’s performance against base-
171 lines in factual outcome prediction and TEE on the real-world hypertension dataset. Notably, **METO**
172 achieves superior performance over the best baseline, registering an average improvement of 5.0% in
173 AUPR and 6.4% in MM-IP.

174 The basic meta-learners, namely the S-learner and T-learner, exhibit diminished performance in com-
175 parison to advanced deep learning-based TEE approaches. This discrepancy is attributed to their inability
176 to adequately process high-dimensional, heterogeneous patient data and to forge precise patient repre-
177 sentations for accurate effect estimation. While deep learning-based methods for binary treatment and
178 outcome scenarios, such as TARNet, show marginal enhancements over meta-learners, they fall short in
179 addressing the intricacies of multiple treatments and outcomes.

180 Methods designed for multiple treatments, like PerfectMatch and MEMENTO, offer advancements over
181 binary treatment and outcome frameworks. However, their rigid model architectures limit their adaptability

182 and generalizability across diverse treatment interactions, rendering their performance inferior to more
183 flexible approaches like TECE-VAE, LR-learner, and TransTEE, which are tailored for complex treatment
184 and outcome mappings.

185 The exceptional efficacy of **METO** is attributed to two main strategies: Firstly, the incorporation of a
186 multi-treatment encoding module for the explicit encoding of multiple treatments, including the specifics
187 of drug combinations and their administration sequencing. This approach is finely tuned to address
188 the real-world complexities encountered with antihypertensive drugs and their combinatory uses. Sec-
189 ondly, **METO** distinctively models varying types of outcomes—distinguishing therapeutic effectiveness
190 from safety outcomes through the proposed outcome type-informed prediction. By acknowledging the
191 inherent differences in their practical implications and the variability in their distribution across the popula-
192 tion, our method adeptly navigates the dual objectives of optimizing disease progression while mitigating
193 safety risks.

194 Population Outcome Comparison

195 We hypothesize that the drug combination recommended by our model based on the estimated treatment
196 effects can effectively prevent the patients from developing severe disease outcomes. To demonstrate
197 this, we compare the prevalence of different disease outcomes against two patient treatment groups:
198 1) model-recommended treatment and 2) actual treatment (different from the model's recommendation).
199 Specifically, we first obtain a group of patients whose actual treatment is different from the model's rec-
200 ommendation. Then we derive a comparison group by involving the most similar patients whose actual
201 treatment matches the model recommendation. We use the baseline patient representations to calculate
202 the similarity via Euclidean distance. Finally, we compute and compare the prevalence of each disease
203 outcome in Fig. 4. We observe that, for a given outcome, the prevalence rate in patients who receive
204 treatments that are different from our recommendation is higher than the average rate baseline, while the
205 prevalence rate of patients who receive the same treatments as our recommendation is lower than the
206 baseline. This illustrates that our model recommends effective treatment strategies (reflecting on lower
207 prevalence rate on all outcomes), and provides potential clinical insights for doctors to decide the optimal
208 drug combinations for patients with hypertension.

209 Ablation Study

210 To demonstrate the significance of individual components within our model, we conducted a compre-
211 hensive ablation study. We explore the performance impact of various model configurations, including
212 (1) **w/o MT**, where the multi-treatment (MT) encoding module is substituted with a generic embedding
213 layer; (2) **w/o TC-A**, which replaces the treatment-covariate co-attention (TC-CoA) with an average pool-
214 ing approach; (3) **w/o MT and TC-A**, which removes both the MT encoding and TC-CoA to understand
215 the combined effect of these two components; (4) **w/o OT**, omitting the informative outcome types (OT) in
216 multi-outcome prediction; (5) **w/o OC-A**, while replaces the outcome-distinctive covariate attention (OC-A)
217 with an average pooling layer. (6) **w/o OT and OC-A** removes both the OT information and TC-CoA.

218 The results in Fig. 5 present model superiority across various configurations. Notably, the **w/o MT**
219 **and TC-A** variant exhibits the most significant performance drop, underscoring the critical role of multi-
220 treatment encoding and treatment-covariate co-attention in effectively capturing the nuanced relationships
221 between treatments and covariates. Similarly, the **w/o OT and OC-A** configuration shows a marked de-
222 crease in performance, highlighting the value of incorporating outcome types and the outcome-distinctive
223 covariate attention mechanism for enhanced prediction accuracy.

224 Further comparisons with nuanced model variants reveal the significance of each individual compo-
225 nent to model performance. For example, **w/o TC-A**, **w/o OC-A**, which employ average pooling instead of
226 the specialized attention mechanisms, reveal that our proposed attention-based approach is more adept
227 at modeling the intricate interplay among covariates, treatments, and outcomes. This finding affirms the
228 attention mechanism's capability to refine TEE by accurately encoding complex relationships within the
229 data. This ablation study not only confirms the integral role of each proposed component in bolstering
230 model performance but also emphasizes the architecture's holistic design in addressing the challenges

231 of TEE with multiple treatments and multiple outcomes. Additional ablation study on propensity score
232 weighting is provided in Appendix Table [A7](#).

233 Case Study

234 **Treatment Recommendation.** Identifying optimal antihypertension drug combinations is inherently com-
235 plex due to the multiple available treatments, various drug combinations, multiple patient outcomes, and
236 patient heterogeneity. Our model addresses this complexity by providing a comprehensive clinical out-
237 come assessment tool that evaluates the effects of various drug combinations on both therapeutic effec-
238 tiveness and safety outcomes. Through a detailed case study depicted in Fig. 6, we demonstrate the
239 practical application of our model in guiding antihypertensive treatment decisions. Within this framework,
240 a patient’s medical record is analyzed to estimate the effects of all potential drug combinations. These
241 estimates are then prioritized according to their effectiveness, with a simultaneous assessment of associ-
242 ated safety risks, providing a comprehensive overview for clinical review. In the illustrated case, the model
243 identified the combination of TZDs and ACEIs initiated simultaneously as the strategy offering the most
244 significant therapeutic benefit and minimum safety concerns. This finding exemplifies the model’s ability to
245 recommend treatment plans that optimize for both efficacy and safety, presenting a valuable assessment
246 and decision-support tool for clinicians.

247 **Attention Visualization.** For investigating the effect of outcome-distinctive covariate attention, we visu-
248 alize the attention weights on the patient pre-treatment covariates using a heatmap in Fig. 7. It presents
249 the top 20 covariates ranked by the learned attention weights of a patient who was prescribed ACEIs
250 and CCBs as initial combination therapy and subsequently developed HF and VTE during their disease
251 progression. This heatmap visualization elucidates the distinct and shared covariate relevancies across
252 the two outcome categories, highlighting how certain conditions such as “respiratory failure; insufficiency;
253 arrest” and “pulmonary heart disease” have high relevance for both HF and VTE. Conversely, specific
254 conditions like “coagulation and hemorrhagic disorders” show a pronounced association primarily with
255 VTE, reflecting the model’s nuanced understanding of different mechanisms of effectiveness and safety
256 outcomes. This analysis confirms the capability of the proposed attention networks to dynamically con-
257 centrate on both unique and shared information pertinent to patient outcomes. By effectively capturing
258 and modeling the intricate relationships between various covariates and outcomes, attention mechanisms
259 play a crucial role in enhancing the model’s predictive accuracy in TEE, thereby supporting personalized
260 treatment strategies.

261 Discussion

262 In this paper, we studied the problem of treatment effect estimation in the complex context of hypertension
263 management, characterized by multiple drug combinations and multiple outcomes. We proposed **METO**,
264 an innovative methodology designed to address these complexities. **METO** employs multi-treatment en-
265 coding to unravel the intricacies of various drug combinations and leverages outcome type information to
266 better differentiate between effectiveness and safety outcomes. Validated by extensive experiments on a
267 real-world dataset, **METO** demonstrates superior performance compared to traditional TEE methods. By
268 offering a more comprehensive treatment effect assessment for antihypertensive drugs, **METO** makes a
269 substantial contribution to improving patient care in the field of hypertension management.

270 **TEE under Multiple Treatments.** Traditional TEE research is largely anchored in binary treatment and
271 binary outcome scenarios^[8-10,25,28], posing challenges when extending to accommodate the complexity
272 of real-world healthcare scenarios involving multiple treatments and multiple outcomes. Though some
273 studies^[11-13] have been proposed to specifically address the challenges of multiple treatments, they often
274 face computational inefficiencies and less flexibility. For instance, MEMENTO^[13], which is a direct exten-
275 sion of a traditional TEE method (TARNet^[8]), assigns covariates from different treatment groups to different
276 branches in their model. This approach can be less flexible with varying numbers of treatments. Meth-
277 ods^[15,16,22] that encode multiple treatments into a hidden embedding space offer some improvements in
278 modeling flexibility. TECE-VAE^[16], for instance, incorporates latent variables and causal structure through

279 a variational autoencoder (VAE), and models multiple treatments with a task embedding. However, all
280 these methods still fall short of fully capturing the complexities of multiple treatments in real applications,
281 where the treatment can be a drug combination with different administration sequences, thus leading to
282 an insufficient understanding of treatments and suboptimal model performance.

283 **TEE under Multiple Outcomes.** Recent approaches^[17-19,22,29] have attempted to address TEE under
284 multiple outcome scenarios. For example, Kennedy et al.^[17] propose to translate the treatment effects of
285 multiple outcomes to a common scale and then estimate these scaled effects with non-parametric statisti-
286 cal methods. Argaw et al.^[19] examine the heterogeneous treatment effects and identify patient subpop-
287 ulations under multiple outcomes. However, most methods are designed and evaluated on randomized
288 controlled trial data (e.g., A/B testing) without the consideration of confounding bias (i.e., non-randomized
289 treatment assignment) that widely exists in observational patient data. More importantly, a crucial aspect
290 in our context is the differentiation between types of outcomes: therapeutic effectiveness versus safety
291 endpoints. The omission of this distinction in current methodologies can lead to inaccuracies in outcome
292 prediction and failure to identify optimal treatment strategies that consider both aspects.

293 **Covariate Balancing Assessment.** In observational studies, it is crucial to ensure that the treatment
294 groups are comparable with respect to baseline characteristics. We achieve this through propensity
295 weighting, which reduces potential confounding by re-weighting each individual based on the propensity
296 score. We compare the covariate balancing of the unweighted (original) and weighted data with absolute
297 standard mean difference (ASMD). The ASMD is a widely used metric in propensity score analysis, quan-
298 tifying the difference in means (or proportions) of a covariate between treatment groups, standardized
299 by the pooled standard deviation. An ASMD of 0.1 or less is generally considered to indicate adequate
300 balance. We follow existing work^[30] to calculate the ASMD of a target treatment against the remaining
301 treatments. Figure 8 presents the ASMD of drug combination cohort “TZDs + ACEIs” for a variety of
302 covariates, including demographic factors (e.g., age), clinical diagnoses (e.g., thyroid disorders, diabetes
303 mellitus with complications), and medications (e.g., furosemide, metformin). In the unweighted original
304 data, several covariates exhibit ASMDs greater than the 0.1 threshold, indicating a significant imbalance.
305 After re-weighting the population, the ASMDs for most covariates are reduced and fall below the 0.1
306 threshold, demonstrating improved balance. This enhanced balance demonstrates that the confound-
307 ing bias is mitigated, ensuring the accuracy of estimated treatment effects. A comprehensive covariate
308 balancing plot for all covariates is provided in Appendix Fig. [A2](#).

309 **Results on Semi-Synthetic Data.** Since ground truth treatment effects are unavailable in observational
310 data (i.e., only one of the potential outcomes can be observed), direct evaluation of model performance
311 for estimation accuracy is not possible. To address this limitation, we conducted experiments on semi-
312 synthetic data with simulated true treatment effects. Specifically, treatment assignments and outcomes
313 were simulated based on real patient covariates (details provided in Appendix [D.1](#)). Comparative results
314 are presented in Appendix Table [A5](#), showing that the proposed model achieves the highest performance
315 across all baselines on the semi-synthetic data.

316 **Potential trade-offs among outcomes.** In our paper, we consider multiple disease outcomes and iden-
317 tify the optimal drug combination as one that achieves both maximum effectiveness and minimal safety
318 risks. However, there are potential trade-offs among outcomes, particularly in cases where the treat-
319 ment option with maximum effectiveness may not align with minimal safety risks. To mitigate this, it is
320 essential to incorporate clinicians’ expert knowledge. In real-world clinical settings, clinicians can help
321 determine the relative importance of different outcomes based on their practical experience and model
322 estimated treatment effects. By integrating clinical insights with model outputs, we can carefully assess
323 and prioritize outcomes, ultimately combining them into a single, composite endpoint that balances both
324 effectiveness and safety considerations. This approach allows for the identification of the optimal treat-
325 ment option based on its estimated effects on the combined outcome, ensuring that the selected treatment
326 best aligns with the patient’s overall needs and preferences.

327 **Limitations of the Study** We acknowledge that our paper has limitations. First, from a data perspec-
328 tive, the use of observational data presents challenges, primarily due to the absence of ground truths for
329 treatment effects. This lack of true benchmarks makes it difficult to directly evaluate the model's accuracy
330 in estimating treatment effects. To address this limitation, we proposed the use of a proxy metric, MM-
331 IP, to approximate estimation error and supplemented our analysis with experiments on a semi-synthetic
332 dataset that includes simulated ground truths. Second, from methodology perspective, in estimating treat-
333 ment effects across multiple outcomes and identifying the optimal treatments, potential conflicts among
334 outcomes may arise. We anticipate that, in real clinical settings, incorporating clinicians' expertise as prior
335 knowledge could help guide the process, minimizing conflicts and enabling convergence toward a reliable
336 recommendation.

337 **Acknowledgments**

338 This work was funded in part by the National Institutes of Health (NIH) under award number R01GM141279.
339 The content is solely the responsibility of the authors and does not necessarily represent the official views
340 of the NIH.

341 **Author contributions**

342 PZ conceived the project. RL and PZ developed the method. RL conducted the experiments. RL, PZ,
343 and LL analyzed the results. RL and PZ wrote the manuscript. All authors read and approved the final
344 manuscript.

345 **Declaration of interests**

346 The authors declare no competing interests.

347 **Resource availability**

348 **Lead contact**

349 Further information and requests for resources should be directed to and will be fulfilled by the lead
350 contact, Dr. Ping Zhang (zhang.10631@osu.edu).

351 **Data and code availability**

352 The data we use is from MarketScan Commercial Claims and Encounters (CCAE) and includes ap-
353 proximately 130 million patients from 2012 to 2021. Access to the MarketScan data analyzed in this
354 manuscript is provided by The Ohio State University. The dataset is available at <https://www.merative.com/real-world-evidence>. The source code for this paper can be downloaded from the GitHub reposi-
355 tory at <https://github.com/ruoqi-liu/METO>.
356

357 **Methods**

358 In this section, we introduce the proposed **METO** framework for treatment effect estimation under multiple
359 treatments and multiple outcomes on observational patient data. Fig. 9 shows an illustration of the
360 proposed framework. Specifically, this framework consists of four modules: patient data encoding, multi-
361 treatment modeling, multi-outcome prediction, and treatment recommendation.

362 Preliminaries

363 **Observational Patient Data.** The observational patient data is denoted as $\{\bar{x}, c, \mathbf{a}, \mathbf{y}\}$. Here, $\bar{x} =$
364 $\{x^1, \dots, x^T\}$ represents the patient's medical history over T timestamps, capturing the details of each
365 medical visit. The variable c stands for static demographic information, including age (categorical) and
366 gender (binary). Each medical visit, x^t , contains a series of medications and diagnosis codes. Specifically,
367 medications are represented as $m_1, \dots, m_{|\mathcal{M}|} \in \mathcal{M}$, where $|\mathcal{M}|$ is the total number of unique medication
368 codes in the dataset. Similarly, diagnosis codes are denoted as $d_1, \dots, d_{|\mathcal{D}|} \in \mathcal{D}$, with $|\mathcal{D}|$ representing the
369 total number of unique diagnosis codes.

370 **Multiple Treatments.** This work studies multiple treatment scenarios for antihypertensive drug combi-
371 nations. Each drug combination is represented as $\mathbf{a}_{i,j}^o$, where (a_i, a_j, o) denotes individual drugs a_i, a_j
372 from the antihypertensive medication set \mathcal{A} , and $o \in \mathcal{O}$ of the treatment assignment order. This order
373 includes initial combination therapy (simultaneous administration of a_i and a_j) and stepped-care protocols
374 (sequential administration of a_i followed by a_j , or vice versa). Let P denote the total number of unique
375 drug combinations.

376 **Multiple Outcomes.** The investigation extends to multiple outcomes, $\mathbf{y} = y_1, \dots, y_K$, where each out-
377 come y_k , binary in nature, relates to a specific aspect of hypertension disease progression. Here, K
378 denotes the total number of distinct outcomes. Each outcome y_k is also associated with a type label
379 g_k , categorizing it as either an effectiveness outcome or a safety outcome. This classification provides a
380 comprehensive view of the treatment's impact, enabling the assessment of treatment effects from different
381 perspectives.

382 **Treatment Effect Estimation.** We extend the Neyman-Rubin potential outcome framework³¹ to accom-
383 modate multiple treatments and multiple outcomes. Given patient pre-treatment covariates \bar{x}, c and dis-
384 tinct treatment combinations $\mathbf{a}_{i,j}^o$ and $\mathbf{a}_{q,r}^s$ with $i, j, q, r \in \mathcal{A}$ and $o, s \in \mathcal{O}$, the conditional average treatment
385 effect (CATE) for the k -th outcome is defined as $\mathbb{E}[y_k(\mathbf{a}_{i,j}^o) - y_k(\mathbf{a}_{q,r}^s) | \bar{x}, c]$. This expression considers
386 $y_k(\mathbf{a}_{i,j}^o)$ and $y_k(\mathbf{a}_{q,r}^s)$ as the potential outcomes under treatment combinations $\mathbf{a}_{i,j}^o$ or $\mathbf{a}_{q,r}^s$, respectively.
387 In observational data, outcomes for the non-received treatments remain unobserved, posing the funda-
388 mental causal inference challenge, distinct from traditional supervised learning. To ensure identifiability
389 of treatment effects from observational data, we adhere to three standard assumptions: consistency,
390 positivity, and ignorability³², as elaborated in Appendix [A](#). Under these premises, the treatment effect is
391 estimated as $\mathbb{E}[y_k | \mathbf{a}_{i,j}^o, \bar{x}, c] - \mathbb{E}[y_k | \mathbf{a}_{q,r}^s, \bar{x}, c]$.

392 Patient Data Encoding

393 The patient data is originally denoted by high-dimensional medical codes with temporal information. To
394 convert such raw patient data into informative patient representations, we propose patient data encoding,
395 which consists of a visit embedding layer and a time-aware Transformer encoder. Below, we integrate
396 mathematical formulations to elucidate the operations within these components.

397 **Visit Embedding Layer.** The visit embedding layer focuses on the patient's covariates in medical history,
398 denoted as $\bar{x} = \{x^1, \dots, x^T\}$. Each element x^t (where $t \in 1, \dots, T$) represents the details of a patient's
399 visit at a specific timestamp. The embedding layer maps these discrete visit records into a continuous
400 vector space, resulting in an embedded representation $e(x^t)$ for each visit. Formally, the embedding of
401 the t -th visit is given by:

$$e(x^t) = \text{VisitEmbeddingLayer}(x^t), \quad \forall t \in 1, \dots, T \quad (2)$$

402 **Time-aware Transformer Encoder.** To enhance the patient representation, time information is also en-
403 coded and integrated with the visit embeddings. Specifically, the time interval (v_t) between the t -th visit
404 and the initiation of treatment is encoded into a time embedding $e(v^t)$, parallel to the visit embeddings as:

$$e(v^t) = \text{TimeEmbeddingLayer}(v^t), \quad \forall t \in 1, \dots, T \quad (3)$$

405 This addition allows the model to account for temporal dynamics explicitly, which are essential in health-
406 care applications. The combined input to the Transformer encoder³³ (see details of Transformer layers in

407 Appendix **B.1**) consists of both visit and time embeddings. Let \mathbf{h}^0 denote the initial hidden representation
408 as below:

$$\mathbf{h}^0 = [e(x^1) + e(v^1), \dots, e(x^T) + e(v^T), e(c)] \quad (4)$$

409 The Transformer processes this enriched input through L layers:

$$\mathbf{h}^l = \text{TransformerEncoderLayer}(\mathbf{h}^{l-1}), \quad l \in 1, \dots, L \quad (5)$$

410 The final output \mathbf{h}^L is a comprehensive representation of the patient, effectively capturing both the tempo-
411 ral aspects of the medical history and static demographic information. This encoded information (denoted
412 as \mathbf{h} for simplicity) is then utilized in subsequent multi-treatment modeling and multi-outcome prediction.

413 Multi-Treatment Modeling

414 This module is designed to address the complexities of multi-treatment modeling, specifically for drug
415 combinations in hypertension management. First, the module encodes multiple drug combinations into
416 latent embeddings. Then, it models the relationships between covariates and treatments to extract
417 treatment-related information. The predicted treatment probability is further utilized as balancing weights
418 to adjust for confounding bias.

419 **Multi-Treatment Encoding.** The initial phase of this module focuses on encoding the drug combinations
420 into an embedding space. Given a drug combination $\mathbf{a}_{i,j}^o$, which includes two individual drugs (a_i and a_j)
421 and their assignment order o , we approach the encoding process in a two-fold manner to capture both the
422 drug-specific information and its sequential information.

423 Firstly, each drug in the combination, a_i and a_j , is encoded separately through a drug embedding layer,
424 which transforms the discrete drug identifiers into continuous vector representations. The embeddings for
425 a_i and a_j are obtained as:

$$\begin{aligned} e(a_i) &= \text{DrugEmbeddingLayer}(a_i), \\ e(a_j) &= \text{DrugEmbeddingLayer}(a_j) \end{aligned} \quad (6)$$

426 The assignment order o , which indicates whether the drugs are administered simultaneously or sequen-
427 tially, is also encoded. The order encoding captures the temporal aspect of the treatment administration.
428 This is represented as:

$$e(o) = \text{OrderEmbeddingLayer}(o) \quad (7)$$

429 Secondly, to achieve a deep fusion of individual drugs and assignment order for a comprehensive
430 treatment representation, we propose a treatment fusion layer:

$$s(\mathbf{a}_{i,j}^o) = \text{TreatmentFusion}(e(a_i), e(a_j), e(o)) \quad (8)$$

431 Specifically, this component first concatenates the drug embeddings with the order embedding and then
432 projects this concatenated vector to a latent space through a fully connected layer (FC) for dimensionality
433 alignment and feature extraction:

$$e(\mathbf{a}_{i,j}^o) = \text{FC}([e(a_i), e(a_j), e(o)]) \quad (9)$$

434 In addition, a self-attention mechanism (multi-head attention mechanism³³) is applied to weigh and inte-
435 grate the information from the drug and order embeddings adaptively:

$$s(\mathbf{a}_{i,j}^o) = \text{SelfAttention}(e(\mathbf{a}_{i,j}^o)) \quad (10)$$

436 **Treatment-Covariate Co-Attention.** This component plays a critical role in modeling the interactions
437 between specific treatments and patient covariates. By considering treatment representation $s(\mathbf{a}_{i,j}^o)$ as
438 “queries” and patient hidden representations \mathbf{h} (last hidden state of transformer encoder) as both “keys”
439 and “values”, we employ a co-attention mechanism³⁴ that dynamically adjusts the focus on relevant co-
440 variates for each treatment option:

$$\mathbf{h}_a = \text{Softmax} \left(s(\mathbf{a}_{i,j}^o) \mathbf{h} / \sqrt{d_k} \right) \mathbf{h} \quad (11)$$

441 where d_k is the dimensionality of the key embeddings. This co-attention mechanism allows the model to
442 dynamically focus on different aspects of the patient’s representation in relation to each treatment.

443 **Treatment Prediction.** The pooled patient representation \mathbf{h}_{pool} (i.e., taking the first [CLS] token from \mathbf{h}) is
444 processed through a fully-connected layer with a sigmoid activation function σ as the last layer to predict
445 the probability of receiving each treatment $\hat{\mathbf{a}}_{i,j}^o$ as follows:

$$\hat{\mathbf{a}}_{i,j}^o = \sigma(\text{FC}(\mathbf{h}_{pool})) \quad (12)$$

446 The treatment prediction task is formulated as a multi-class classification problem, where each class
447 corresponds to a specific treatment combination. The treatment prediction loss function is defined as:

$$\mathcal{L}_{\text{treat}} = - \sum_{i,j \in \mathcal{A}, o \in \mathcal{O}} \mathbf{a}_{i,j}^o \log(\hat{\mathbf{a}}_{i,j}^o) \quad (13)$$

448 where $\mathbf{a}_{i,j}^o$ is the ground truth treatment assignment. By minimizing $\mathcal{L}_{\text{treat}}$, the model is optimized to predict
449 the probability of receiving each treatment combination.

450 **Propensity Score Weighting.** The predicted probability of receiving treatment, also known as the
451 propensity score³⁵, is further leveraged to reduce the bias from confounding factors. Specifically, the
452 balancing weights can be derived from the propensity scores and then used to estimate the potential
453 outcomes. The inverse probability of treatment weighting (IPTW)³⁶ is employed and extended to multiple
454 treatment settings³⁷ as follows,

$$w = \frac{W(\mathbf{a}_{i,j}^o)}{\hat{\mathbf{a}}_{i,j}^o} \quad (14)$$

455 where $W(\mathbf{a}_{i,j}^o)$ is the marginal probability of treatment $\mathbf{a}_{i,j}^o$ that is included to stabilize the weights³⁸. Then
456 the weight is used in the multi-outcome prediction to re-weight the patient and adjust for confounding bias.

457 Multi-Outcome Prediction

458 This module focuses on predicting multiple disease outcomes in a nuanced and comprehensive manner.
459 This module first encodes the distinctive relationships among different outcomes and patient covariates
460 and then predicts the outcomes, weighted based on the balancing propensity scores.

461 **Outcome-Distinctive Covariate Attention.** This component addresses the distinctive impact that patient
462 covariates have on different disease outcomes. It computes an outcome-distinctive covariate attention
463 score $\alpha \in \mathbb{R}^{K \times N}$ (where K is the number of outcomes, and N is the length of patient sequence) as
464 follows:

$$\begin{aligned} \alpha &= \text{softmax}(W_2 \tanh(W_1 \tilde{\mathbf{h}}^T)) \\ \tilde{\mathbf{h}} &= \text{MLP}([\mathbf{h}_a, \mathbf{h}]) \end{aligned} \quad (15)$$

465 where, $W_1 \in \mathbb{R}^{d_o \times d_h}$ and $W_2 \in \mathbb{R}^{K \times d_o}$ are trainable weight matrices, $\alpha_{k,n}$ (each element of α) indicates the
466 contribution of the n -th covariate to the k -th outcome. Leveraging α , the mechanism produces outcome-
467 distinctive patient representations as $\mathbf{h}_o = \alpha \mathbf{h}$, thereby refining the predictions for each distinct outcome.

468 **Re-weighted Multi-outcome Prediction with Type Information.** We recognize the critical role of out-
469 come type (i.e., distinguishing between effectiveness and safety) in accurately predicting patient re-
470 sponses to treatment. These types embody the dual (opposing) aspects of patient outcomes, each critical
471 to understanding the full scope of treatment impacts. To harness this crucial insight, we propose first to
472 predict each outcome type, \hat{g}_k , utilizing this prediction to enhance the subsequent outcome prediction, \hat{y}_k .
473 In a teacher-forcing-like approach, during the training, the model predominantly uses the actual outcome
474 types g_k as supplementary context for enhancing outcome predictions, while in testing, it relies on its
475 predictive capabilities for \hat{g}_k . Formally, we have

$$\hat{g}_k = \sigma(f_g(\mathbf{h}_o)), \quad \hat{y}_k = \sigma(f_\eta(\mathbf{h}_o, g_k, \hat{g}_k)) \quad (16)$$

476 Here, f_g denotes the function to predict outcome type. f_η is the function to predict the outcome itself,
477 where $\eta \in [0, 1]$ represents a tunable probability parameter designed to modulate the dependency on true
478 versus predicted outcome types.

479 To address the potential issue of positive-negative imbalance encountered in outcome prediction (i.e.,
480 where the incidence rate of certain disease outcomes may be notably low), we employ the Asymmetric
481 Loss (ASL)³⁹. ASL is adept at handling such imbalances by calculating separate losses for positive and
482 negative samples, denoted as \mathcal{L}_+ and \mathcal{L}_- , respectively. The formulation is as follows:

$$\mathcal{L}_{\text{outcome}} = \begin{cases} \mathcal{L}_+ = w(1 - \hat{y})^{\gamma_+} \log(\hat{y}) \\ \mathcal{L}_- = w\hat{y}^{c\gamma_-} \log(1 - \hat{y}^c) \end{cases} \quad (17)$$

483 where $\hat{y}^c = \max(\hat{y} - c, 0)$ represents the adjusted outcome probability for negative examples, incorporating
484 a margin c for hard thresholding. The hyperparameters γ_-, γ_+ are set such that $\gamma_- \leq \gamma_+$, enabling ASL
485 to appropriately down-weight and apply hard thresholds to easy negative samples, thereby mitigating
486 the imbalances. The balancing weight, w (from Eq. 14), is introduced to adjust the importance of each
487 sample in the loss function based on the treatment assignment probability, which helps to mitigate the
488 bias introduced by the non-random treatment assignment.

489 **Optimization and Treatment Effect Estimation.** The overall loss function integrates the outcome pre-
490 diction loss $\mathcal{L}_{\text{outcome}}$ with the treatment prediction loss $\mathcal{L}_{\text{treat}}$ as:

$$\mathcal{L} = \mathcal{L}_{\text{outcome}} + \lambda \mathcal{L}_{\text{treat}} \quad (18)$$

491 where λ is a weighting factor that balances the importance of the outcome prediction loss and the treat-
492 ment prediction loss. This combined loss function ensures that the model is trained to accurately predict
493 both patient outcomes and treatment assignments, reflecting the complex relations of treatments and their
494 effects.

495 The estimated treatment effect under a pair of treatments $\mathbf{a}_{i,j}^o$ and $\mathbf{a}_{q,r}^s$ is defined as the differential
496 between the potential outcomes:

$$\hat{y}_k(\mathbf{a}_{i,j}^o) - \hat{y}_k(\mathbf{a}_{q,r}^s), \quad \forall k \in 1, \dots, K \quad (19)$$

497 This estimation is essential for elucidating the comparative impact of different treatments, thereby equip-
498 ping healthcare professionals with the insights needed to make informed treatment selections.

499 Treatment Recommendation

500 This module demonstrates the application of the proposed **METO** in a healthcare problem for antihy-
501 pertensive drug combination recommendation. Utilizing the estimated treatment effects across diverse
502 drug combinations facilitates the identification of an optimal treatment strategy with maximum therapeutic
503 efficacy and minimum drug safety concerns.

504 Specifically, the trained model, f_{θ^*} , with θ^* representing the optimized parameters, is employed to si-
505 multaneously evaluate effectiveness and safety outcomes for each potential treatment regimen concerning
506 a new patient as:

$$\hat{y}_k(\mathbf{a}_{i,j}^o) = f_{\theta^*}(\bar{\mathbf{x}}, c, \mathbf{a}_{i,j}^o), \quad \forall k \in 1, \dots, K \quad (20)$$

507 The model evaluates each antihypertensive drug combination $\mathbf{a}_{i,j}^o$ by predicting effectiveness outcomes,
508 $\hat{y}_{\text{effect}}(\mathbf{a}_{i,j}^o)$, and safety outcomes, $\hat{y}_{\text{safe}}(\mathbf{a}_{i,j}^o)$. The therapeutic effectiveness improvement over a baseline,
509 denoted as $\hat{\tau}_{\text{effect}}(\mathbf{a}_{i,j}^o) = \hat{y}_{\text{effect}}(\mathbf{a}_{i,j}^o) - \hat{y}_{\text{base}}$, guides the ranking of treatments. The optimal treatment, $\mathbf{a}_{\text{opt}}^*$,
510 is then identified as the one offering maximal effectiveness improvement while ensuring minimal safety
511 risk:

$$\mathbf{a}_{\text{opt}}^* = \underset{i,j \in \mathcal{A}, o \in \mathcal{O}}{\operatorname{argmin}} \hat{y}_{\text{safe}}(\mathbf{a}_{i,j}^o) \text{ s.t. } \max_{i,j \in \mathcal{A}, o \in \mathcal{O}} \hat{\tau}_{\text{effect}}(\mathbf{a}_{i,j}^o) \quad (21)$$

512 This streamlined approach empowers healthcare professionals to tailor treatment plans precisely, balanc-
513 ing efficacy with safety, to meet individual patient needs effectively.

514 References

- 515 1. Rojas Rueda, D. (2017). Global burden of hypertension and systolic blood pressure of at least 110
516 to 115 mm hg, 1990-2015. *JAMA*, 2017, vol. 317, num. 2, p. 165-182.
- 517 2. Frank, J. (2008). Managing hypertension using combination therapy. *American family physician* 77,
518 1279–1286.
- 519 3. Whelton, P. K., Carey, R. M., Aronow, W. S., Casey, D. E., Collins, K. J., Dennison Him-
520 melfarb, C., DePalma, S. M., Gidding, S., Jamerson, K. A., Jones, D. W. et al. (2018). 2017
521 acc/aha/aapa/abc/acpm/ags/apha/ash/aspc/nma/pcna guideline for the prevention, detection, evalu-
522 ation, and management of high blood pressure in adults: a report of the american college of cardi-
523 ology/american heart association task force on clinical practice guidelines. *Journal of the American*
524 *College of Cardiology* 71, e127–e248.
- 525 4. Mancia, G., Rea, F., Corrao, G., and Grassi, G. (2019). Two-drug combinations as first-step antihy-
526 pertensive treatment. *Circulation research* 124, 1113–1123.
- 527 5. Lu, Y., Van Zandt, M., Liu, Y., Li, J., Wang, X., Chen, Y., Chen, Z., Cho, J., Dorajoo, S. R., Feng, M.
528 et al. (2022). Analysis of dual combination therapies used in treatment of hypertension in a multina-
529 tional cohort. *JAMA network open* 5, e223877–e223877.
- 530 6. Suchard, M. A., Schuemie, M. J., Krumholz, H. M., You, S. C., Chen, R., Pratt, N., Reich, C. G., Duke,
531 J., Madigan, D., Hripcsak, G. et al. (2019). Comprehensive comparative effectiveness and safety of
532 first-line antihypertensive drug classes: a systematic, multinational, large-scale analysis. *The Lancet*
533 394, 1816–1826.
- 534 7. Berkey, C., Anderson, J., and Hoaglin, D. (1996). Multiple-outcome meta-analysis of clinical trials.
535 *Statistics in medicine* 15, 537–557.
- 536 8. Shalit, U., Johansson, F. D., and Sontag, D. A. (2017). Estimating individual treatment effect:
537 generalization bounds and algorithms. In: Precup, D., and Teh, Y. W., eds. *Proceedings of the*
538 *34th International Conference on Machine Learning, ICML 2017, Sydney, NSW, Australia, 6-11*
539 *August 2017 vol. 70 of Proceedings of Machine Learning Research*. PMLR (3076–3085). URL:
540 <http://proceedings.mlr.press/v70/shalit17a.html>.
- 541 9. Shi, C., Blei, D. M., and Veitch, V. (2019). Adapting neural networks for the estimation of treat-
542 ment effects. In: Wallach, H. M., Larochelle, H., Beygelzimer, A., d'Alché-Buc, F., Fox, E. B.,
543 and Garnett, R., eds. *Advances in Neural Information Processing Systems 32: Annual Confer-*
544 *ence on Neural Information Processing Systems 2019, NeurIPS 2019, December 8-14, 2019, Van-*
545 *couver, BC, Canada.* (2503–2513). URL: [https://proceedings.neurips.cc/paper/2019/hash/](https://proceedings.neurips.cc/paper/2019/hash/8fb5f8be2aa9d6c64a04e3ab9f63f6ee-Abstract.html)
546 [8fb5f8be2aa9d6c64a04e3ab9f63f6ee-Abstract.html](https://proceedings.neurips.cc/paper/2019/hash/8fb5f8be2aa9d6c64a04e3ab9f63f6ee-Abstract.html).
- 547 10. Curth, A., and van der Schaar, M. (2021). Nonparametric estimation of heterogeneous treatment
548 effects: From theory to learning algorithms. In: Banerjee, A., and Fukumizu, K., eds. *The 24th*
549 *International Conference on Artificial Intelligence and Statistics, AISTATS 2021, April 13-15, 2021,*
550 *Virtual Event vol. 130 of Proceedings of Machine Learning Research*. PMLR (1810–1818). URL:
551 <http://proceedings.mlr.press/v130/curth21a.html>.
- 552 11. Schwab, P., Linhardt, L., and Karlen, W. (2018). Perfect match: A simple method for learning repre-
553 sentations for counterfactual inference with neural networks. *ArXiv preprint abs/1810.00656*. URL:
554 <https://arxiv.org/abs/1810.00656>.
- 555 12. Parbhoo, S., Bauer, S., and Schwab, P. (2021). Ncore: Neural counterfactual representation learn-
556 ing for combinations of treatments. *ArXiv preprint abs/2103.11175*. URL: [https://arxiv.org/abs/](https://arxiv.org/abs/2103.11175)
557 [2103.11175](https://arxiv.org/abs/2103.11175).

- 558 13. Mondal, A., Majumder, A., and Chaoji, V. (2022). Memento: Neural model for estimating individual
559 treatment effects for multiple treatments. In: Proceedings of the 31st ACM International Conference
560 on Information & Knowledge Management. (3381–3390).
- 561 14. Chu, Z., Rathbun, S. L., and Li, S. (2022). Multi-task adversarial learning for treatment effect estima-
562 tion in basket trials. In: Conference on health, inference, and learning. PMLR (79–91).
- 563 15. Zhang, Y.-F., Zhang, H., Lipton, Z. C., Li, L. E., and Xing, E. P. (2022). Can transformers be strong
564 treatment effect estimators? ArXiv preprint *abs/2202.01336*. URL: [https://arxiv.org/abs/2202.](https://arxiv.org/abs/2202.01336)
565 [01336](https://arxiv.org/abs/2202.01336).
- 566 16. Saini, S. K., Dhamnani, S., Srinivasan, A., Ibrahim, A. A., and Chavan, P. (2019). Multiple treat-
567 ment effect estimation using deep generative model with task embedding. In: Liu, L., White, R. W.,
568 Mantrach, A., Silvestri, F., McAuley, J. J., Baeza-Yates, R., and Zia, L., eds. The World Wide Web
569 Conference, WWW 2019, San Francisco, CA, USA, May 13-17, 2019. ACM (1601–1611). URL:
570 <https://doi.org/10.1145/3308558.3313744>. doi:[10.1145/3308558.3313744](https://doi.org/10.1145/3308558.3313744).
- 571 17. Kennedy, E. H., Kangovi, S., and Mitra, N. (2019). Estimating scaled treatment effects with multiple
572 outcomes. *Statistical methods in medical research* 28, 1094–1104.
- 573 18. Yuki, S., Tanioka, K., and Yadohisa, H. (2021). Estimation and visualization of treatment effects for
574 multiple outcomes. ArXiv preprint *abs/2108.00163*. URL: <https://arxiv.org/abs/2108.00163>.
- 575 19. Argaw, P. N., Healey, E., and Kohane, I. S. (2022). Identifying heterogeneous treatment effects in
576 multiple outcomes using joint confidence intervals. In: Machine Learning for Health. PMLR (141–
577 170).
- 578 20. Sever, P. S., and Messerli, F. H. (2011). Hypertension management 2011: optimal combination ther-
579 apy. *European heart journal* 32, 2499–2506.
- 580 21. Künzel, S. R., Sekhon, J. S., Bickel, P. J., and Yu, B. (2019). Metalearners for estimating heteroge-
581 neous treatment effects using machine learning. *Proceedings of the national academy of sciences*
582 116, 4156–4165.
- 583 22. Yao, L., Lo, C., Nir, I., Tan, S., Evnine, A., Lerer, A., and Peysakhovich, A. (2022). Efficient heteroge-
584 neous treatment effect estimation with multiple experiments and multiple outcomes. ArXiv preprint
585 *abs/2206.04907*. URL: <https://arxiv.org/abs/2206.04907>.
- 586 23. Hill, J. L. (2011). Bayesian nonparametric modeling for causal inference. *Journal of Computational*
587 *and Graphical Statistics* 20, 217–240.
- 588 24. Alaa, A. M., and van der Schaar, M. (2019). Validating causal inference models via influence func-
589 tions. In: Chaudhuri, K., and Salakhutdinov, R., eds. Proceedings of the 36th International Confer-
590 ence on Machine Learning, ICML 2019, 9-15 June 2019, Long Beach, California, USA vol. 97 of
591 *Proceedings of Machine Learning Research*. PMLR (191–201). URL: [http://proceedings.mlr.](http://proceedings.mlr.press/v97/alaa19a.html)
592 [press/v97/alaa19a.html](http://proceedings.mlr.press/v97/alaa19a.html).
- 593 25. Johansson, F. D., Shalit, U., and Sontag, D. A. (2016). Learning representations for counter-
594 factual inference. In: Balcan, M., and Weinberger, K. Q., eds. Proceedings of the 33rd Inter-
595 national Conference on Machine Learning, ICML 2016, New York City, NY, USA, June 19-24,
596 2016 vol. 48 of *JMLR Workshop and Conference Proceedings*. JMLR.org (3020–3029). URL:
597 <http://proceedings.mlr.press/v48/johansson16.html>.
- 598 26. Yao, L., Li, S., Li, Y., Huai, M., Gao, J., and Zhang, A. (2018). Representation learning for treatment
599 effect estimation from observational data. In: Bengio, S., Wallach, H. M., Larochelle, H., Grauman,
600 K., Cesa-Bianchi, N., and Garnett, R., eds. Advances in Neural Information Processing Systems 31:
601 Annual Conference on Neural Information Processing Systems 2018, NeurIPS 2018, December 3-
602 8, 2018, Montréal, Canada. (2638–2648). URL: [https://proceedings.neurips.cc/paper/2018/](https://proceedings.neurips.cc/paper/2018/hash/a50abba8132a77191791390c3eb19fe7-Abstract.html)
603 [hash/a50abba8132a77191791390c3eb19fe7-Abstract.html](https://proceedings.neurips.cc/paper/2018/hash/a50abba8132a77191791390c3eb19fe7-Abstract.html).

- 604 27. Hassanpour, N., and Greiner, R. (2020). Learning disentangled representations for counterfactual regression. In: 8th International Conference on Learning Representations, ICLR 2020, Addis
605 Ababa, Ethiopia, April 26-30, 2020. OpenReview.net. URL: [https://openreview.net/forum?id=](https://openreview.net/forum?id=HkxBJT4YvB)
606 [HkxBJT4YvB](https://openreview.net/forum?id=HkxBJT4YvB).
607
- 608 28. Curth, A., and van der Schaar, M. (2021). On inductive biases for heterogeneous treatment effect estimation. In: Ranzato, M., Beygelzimer, A., Dauphin, Y. N., Liang, P., and
609 Vaughan, J. W., eds. Advances in Neural Information Processing Systems 34: Annual Conference on Neural Information Processing Systems 2021, NeurIPS 2021, December 6-14,
610 2021, virtual. (15883–15894). URL: [https://proceedings.neurips.cc/paper/2021/hash/](https://proceedings.neurips.cc/paper/2021/hash/8526e0962a844e4a2f158d831d5fddf7-Abstract.html)
611 [8526e0962a844e4a2f158d831d5fddf7-Abstract.html](https://proceedings.neurips.cc/paper/2021/hash/8526e0962a844e4a2f158d831d5fddf7-Abstract.html).
612
613
- 614 29. Wu, H., Tan, S., Li, W., Garrard, M., Obeng, A., Dimmery, D., Singh, S., Wang, H., Jiang, D., and
615 Bakshy, E. (2022). Interpretable personalized experimentation. In: Proceedings of the 28th ACM SIGKDD Conference on Knowledge Discovery and Data Mining. (4173–4183).
616
- 617 30. McCaffrey, D. F., Griffin, B. A., Almirall, D., Slaughter, M. E., Ramchand, R., and Burgette, L. F.
618 (2013). A tutorial on propensity score estimation for multiple treatments using generalized boosted
619 models. *Statistics in medicine* 32, 3388–3414.
- 620 31. Rubin, D. B. (2005). Causal inference using potential outcomes: Design, modeling, decisions. *Journal of the American Statistical Association* 100, 322–331.
621
- 622 32. Imbens, G. W., and Rubin, D. B. Causal inference in statistics, social, and biomedical sciences.
623 Cambridge University Press (2015).
- 624 33. Vaswani, A., Shazeer, N., Parmar, N., Uszkoreit, J., Jones, L., Gomez, A. N., Kaiser, L., and Polosukhin, I. (2017). Attention is all you need. In: Guyon, I., von Luxburg, U., Bengio, S., Wallach, H. M.,
625 Fergus, R., Vishwanathan, S. V. N., and Garnett, R., eds. Advances in Neural Information Processing Systems 30: Annual Conference on Neural Information Processing Systems 2017, December
626 4-9, 2017, Long Beach, CA, USA. (5998–6008). URL: [https://proceedings.neurips.cc/paper/](https://proceedings.neurips.cc/paper/2017/hash/3f5ee243547dee91fbd053c1c4a845aa-Abstract.html)
627 [2017/hash/3f5ee243547dee91fbd053c1c4a845aa-Abstract.html](https://proceedings.neurips.cc/paper/2017/hash/3f5ee243547dee91fbd053c1c4a845aa-Abstract.html).
628
629
- 630 34. Murahari, V., Batra, D., Parikh, D., and Das, A. (2020). Large-scale pretraining for visual dialog: A
631 simple state-of-the-art baseline. In: European Conference on Computer Vision. Springer (336–352).
- 632 35. Rosenbaum, P. R., and Rubin, D. B. (1983). The central role of the propensity score in observational
633 studies for causal effects. *Biometrika* 70, 41–55.
- 634 36. Hirano, K., Imbens, G. W., and Ridder, G. (2003). Efficient estimation of average treatment effects
635 using the estimated propensity score. *Econometrica* 71, 1161–1189.
- 636 37. Austin, P. C. (2018). Assessing the performance of the generalized propensity score for estimating
637 the effect of quantitative or continuous exposures on binary outcomes. *Statistics in medicine* 37,
638 1874–1894.
- 639 38. Xu, S., Ross, C., Raebel, M. A., Shetterly, S., Blanchette, C., and Smith, D. (2010). Use of stabilized
640 inverse propensity scores as weights to directly estimate relative risk and its confidence intervals.
641 *Value in Health* 13, 273–277.
- 642 39. Ridnik, T., Baruch, E. B., Zamir, N., Noy, A., Friedman, I., Protter, M., and Zelnik-Manor, L. (2021).
643 Asymmetric loss for multi-label classification. In: 2021 IEEE/CVF International Conference on Computer Vision, ICCV 2021, Montreal, QC, Canada, October 10-17, 2021. IEEE (82–91). URL:
644 <https://doi.org/10.1109/ICCV48922.2021.00015> doi:[10.1109/ICCV48922.2021.00015](https://doi.org/10.1109/ICCV48922.2021.00015)
645
- 646 40. Chen, T., and Guestrin, C. (2016). Xgboost: A scalable tree boosting system. In: Krishnapuram,
647 B., Shah, M., Smola, A. J., Aggarwal, C. C., Shen, D., and Rastogi, R., eds. Proceedings of the

648

649

650

22nd ACM SIGKDD International Conference on Knowledge Discovery and Data Mining, San Francisco, CA, USA, August 13-17, 2016. ACM (785–794). URL: <https://doi.org/10.1145/2939672.2939785>. doi:[10.1145/2939672.2939785](https://doi.org/10.1145/2939672.2939785).

651 **Main tables and corresponding titles and legends**

Table 1: Performance comparison for factual outcome prediction (AUPR) and treatment effect estimation (MM-IP: IF-PEHE for multiple treatments and multiple outcomes). The results are averaged over 20 random runs. Full results with standard deviations for all methods are provided in Appendix Table [A6](#)

| Method | Stroke | | MI | | HF | | AKF | | Gout | | VTE | |
|----------------|--------------|--------------|--------------|--------------|--------------|--------------|--------------|--------------|--------------|--------------|--------------|--------------|
| | AUPR ↑ | MM-IP ↓ | AUPR ↑ | MM-IP ↓ | AUPR ↑ | MM-IP ↓ | AUPR ↑ | MM-IP ↓ | AUPR ↑ | MM-IP ↓ | AUPR ↑ | MM-IP ↓ |
| S-learner | 0.551 | 0.284 | 0.188 | 0.355 | 0.329 | 0.378 | 0.218 | 0.370 | 0.339 | 0.325 | 0.274 | 0.356 |
| T-learner | 0.544 | 0.297 | 0.181 | 0.360 | 0.325 | 0.386 | 0.212 | 0.377 | 0.331 | 0.332 | 0.267 | 0.363 |
| TARNet | 0.569 | 0.271 | 0.196 | 0.351 | 0.342 | 0.357 | 0.233 | 0.359 | 0.349 | 0.318 | 0.288 | 0.355 |
| DragonNet | 0.574 | 0.262 | 0.198 | 0.344 | 0.351 | 0.338 | 0.251 | 0.342 | 0.356 | 0.303 | 0.294 | 0.332 |
| PerfectMatch | 0.591 | 0.239 | 0.202 | 0.361 | 0.388 | 0.312 | 0.274 | 0.331 | 0.378 | 0.289 | 0.312 | 0.317 |
| MEMENTO | 0.584 | 0.244 | 0.208 | 0.354 | 0.382 | 0.317 | 0.270 | 0.338 | 0.372 | 0.294 | 0.310 | 0.322 |
| TECE-VAE | 0.605 | 0.230 | 0.211 | 0.355 | 0.397 | 0.302 | 0.290 | 0.325 | 0.381 | 0.283 | 0.319 | 0.309 |
| LR-learner | 0.609 | 0.225 | 0.206 | 0.364 | 0.392 | 0.308 | 0.296 | 0.321 | 0.385 | 0.280 | 0.326 | 0.315 |
| TransTEE | 0.617 | 0.221 | 0.235 | 0.321 | 0.409 | 0.284 | 0.303 | 0.311 | 0.403 | 0.261 | 0.338 | 0.276 |
| NCoRE | 0.577 | 0.249 | 0.207 | 0.361 | 0.388 | 0.313 | 0.275 | 0.334 | 0.370 | 0.297 | 0.311 | 0.326 |
| METO | 0.656 | 0.185 | 0.329 | 0.225 | 0.442 | 0.236 | 0.364 | 0.238 | 0.453 | 0.204 | 0.363 | 0.201 |
| (<i>std</i>) | 0.011 | 0.003 | 0.009 | 0.005 | 0.013 | 0.004 | 0.014 | 0.007 | 0.007 | 0.006 | 0.008 | 0.003 |

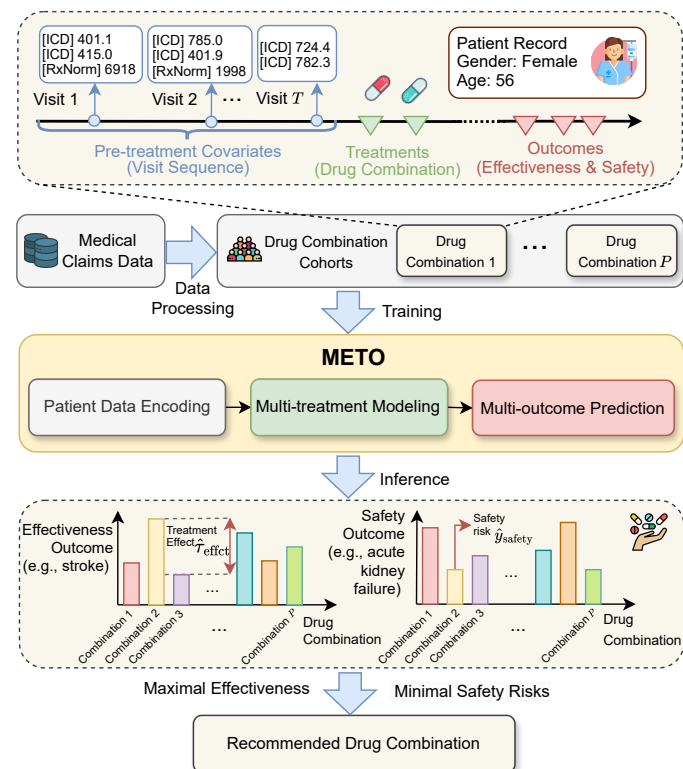


Figure 1: Workflow overview of the proposed **METO**. Patient records are extracted from medical claims data and processed to train the model, which learns to estimate the treatment effects of multiple drug combinations. The lower panel shows the model's output, where the estimated effects on both effectiveness and safety outcomes assist clinicians in making informed treatment decisions for hypertension.

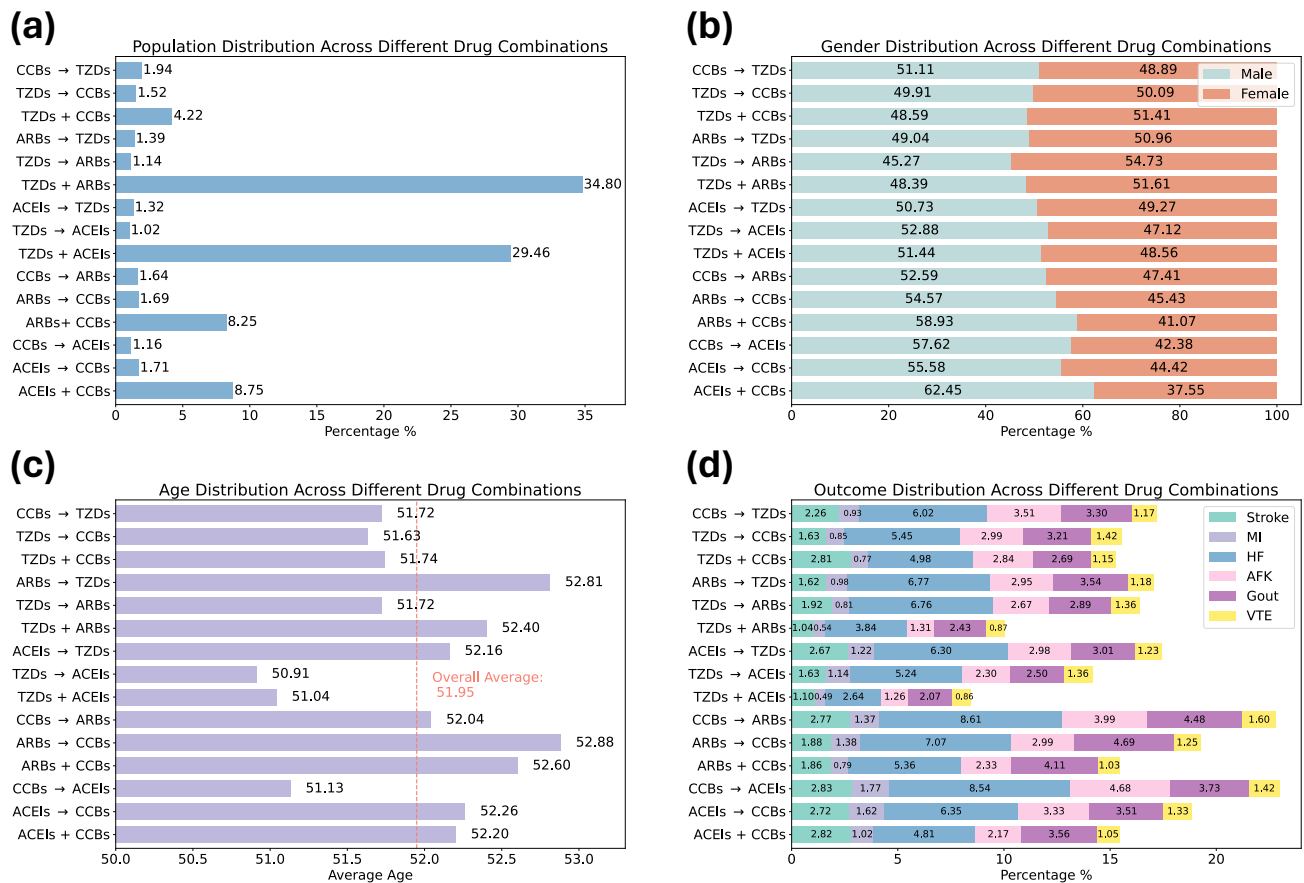


Figure 2: Statistics of hypertension patient cohorts across 15 unique drug combinations. (a) Patient population distribution across different drug combinations. (b) Gender distribution across different drug combinations. (c) Age distribution across different drug combinations. (d) Outcome distribution across different drug combinations. TZDs: thiazide diuretics. ACEIs: ACE inhibitors. ARBs: angiotensin receptor blockers. CCBs: calcium channel blockers. + and → denote the initial combination and stepped-care, respectively (e.g., “ACEIs + CCBs” represents the initial combination of ACEIs and CCBs, while “ACEIs → CCBs” represents first ACEIs, then CCBs sequentially). MI: acute myocardial infarction. HF: heart failure. AFK: acute kidney failure. VTE: venous thromboembolism

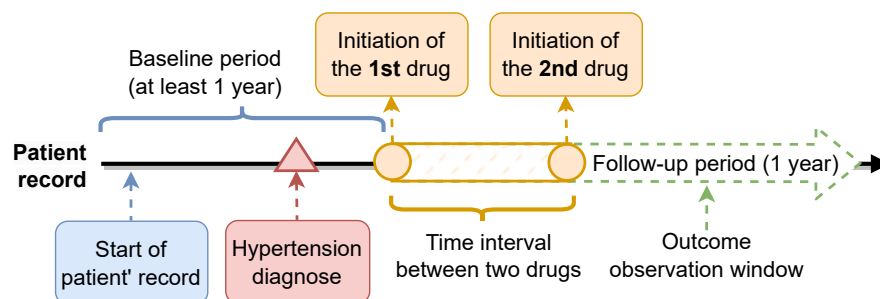


Figure 3: Illustration of the treatment cohort definitions. The treatment consists of two drugs as a combination. The outcomes are computed in the follow-up period. The pre-treatment covariates obtained from the baseline period are regarded as confounders for adjustment.

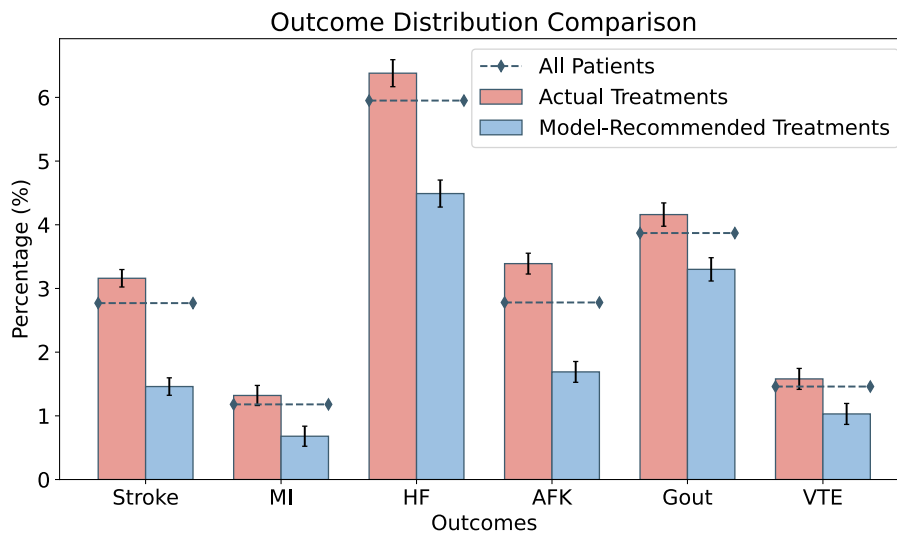


Figure 4: Comparison of disease outcomes for different treatment approaches among the patient population. The percentage of patients experiencing specific outcomes across three categories: all patients (dashed line with diamond markers), actual treatments administered (red bars), and model-recommended treatments (blue bars). The error bars on each column indicate the standard errors of the data points.

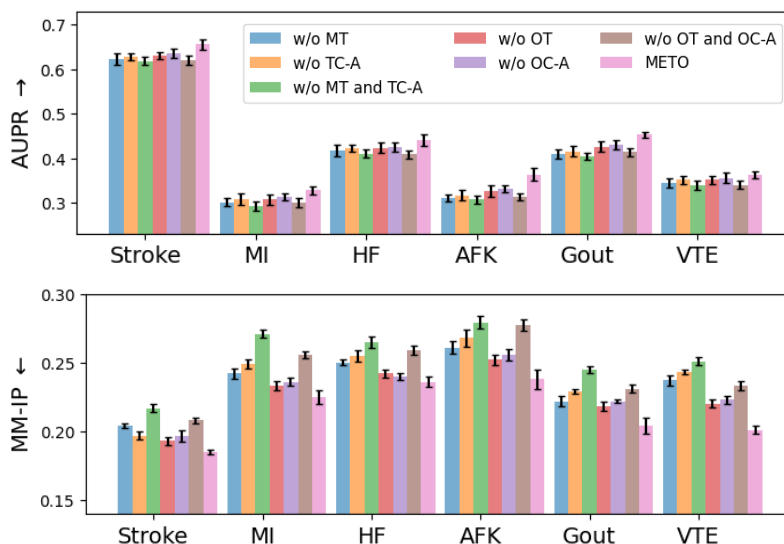


Figure 5: Ablation study for different variants of **METO**. The error bars on each column indicate the standard errors of the data points.

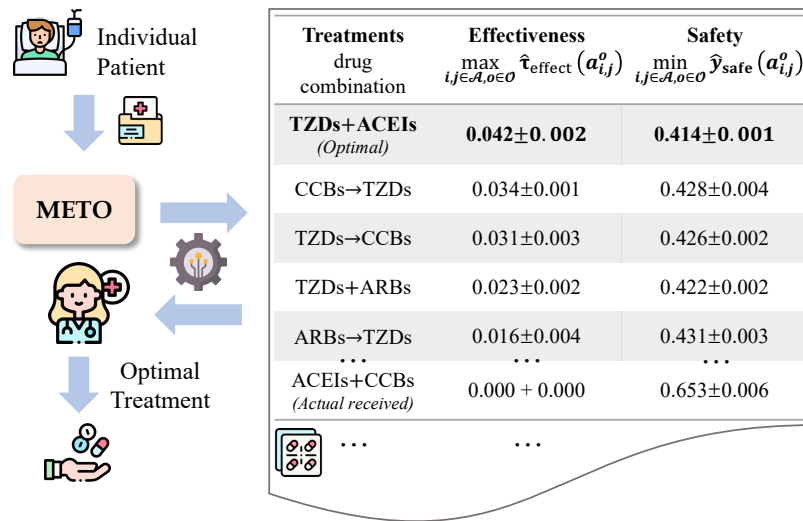


Figure 6: Illustration of how the proposed **METO** can be used to assist clinicians decide the personalized optimal drug combination with beneficial effects and reduced safety risks.

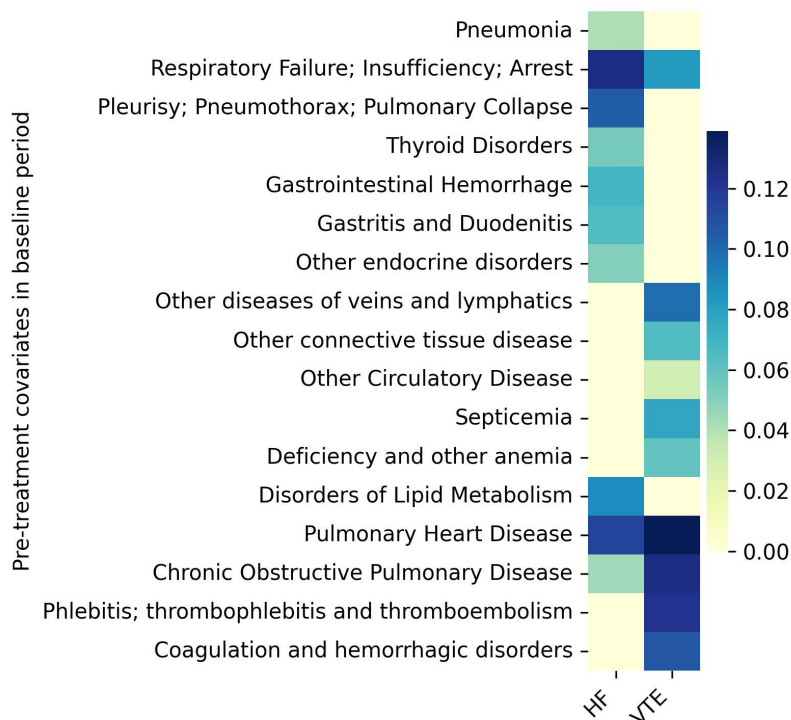


Figure 7: Visualization of covariates with largest outcome-distinctive covariate attention (α_k) of one patient with two outcomes: HF and VTE.

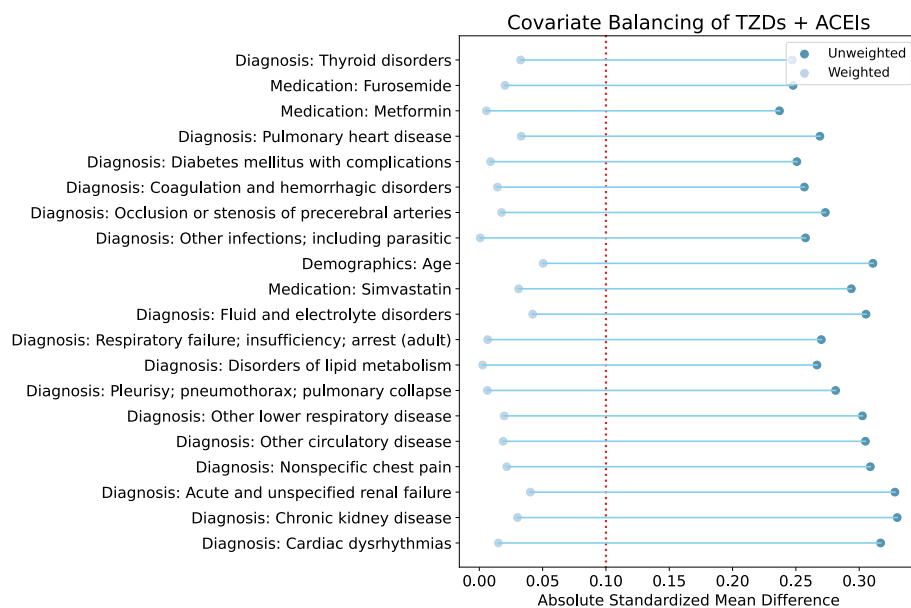


Figure 8: Performance of covariate balancing of TZDs and ACEIs. The absolute standard mean difference (ASMD) values of the top 20 well-balanced covariates before and after weighting are presented. The vertical dotted red line at 0.10 represents the threshold for balance, with points closer to zero indicating better balance.

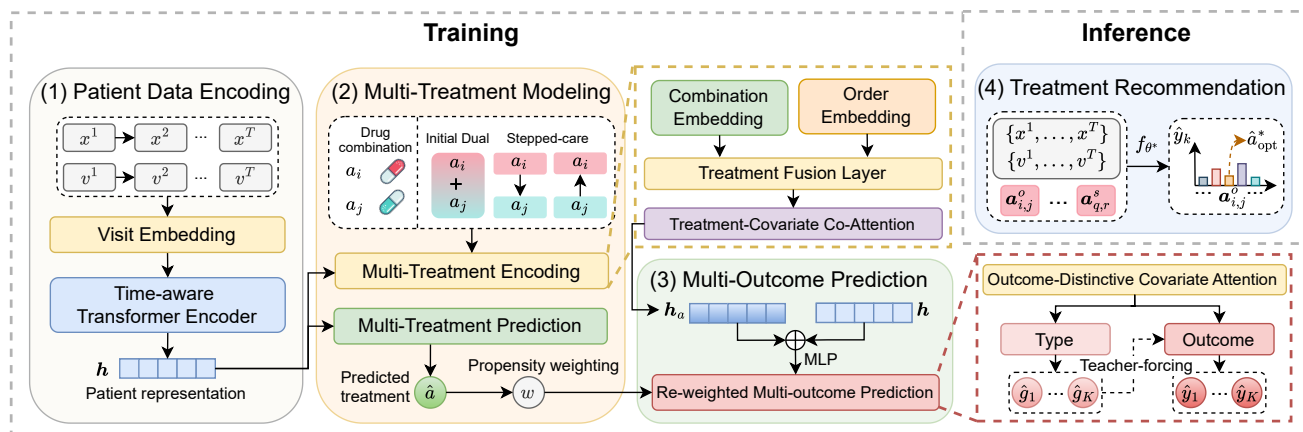


Figure 9: A detailed illustration of **METO**. (1) Patient data encoding: raw patient data is transformed into enriched patient representations. (2) Multi-treatment modeling: drug combinations and administration sequences are encoded, and the probability of receiving each treatment is predicted as balancing scores. (3) Multi-outcome prediction: multiple outcomes are predicted by integrating the patient representations with the treatment representations, re-weighted by the balancing scores. (4) Treatment recommendation: optimal drug combinations are identified based on the estimated treatment effects.